THE DEVELOPMENT OF A NEW MAXIMUM POWER POINT TRACKER FOR A PV PANEL

M. Salhi, R. El-Bachtiri*, E. Matagne***

*REPEER Group, LESSI laboratory, Faculty of sciences dhar el-Mehrez, USMBA University
Higher school of technology, km5, R^{te} Imouzzer, BP 2427, Fez, Morocco.
Telephone: +212 35 600584/Fax: +212 35 600588
E-mail: Salhi_estf@yahoo.fr; bachtri@yahoo.fr

**LEI laboratory, Université Catholique de Louvain
Louvain-la-Neuve, Belgium
E-mail: Ernest.matagne@uclouvain.be

Received: 21 Sept 2007; accepted: 29 Oct 2007

The PV systems are rapidly expanding and have increasing roles in electric power technologies, providing more secure power sources and pollution free electric supplies. Since the PV electricity is expensive compared to the electricity from the utility grid, users want to use all the available output PV power. Therefore, the PV systems should be designed to operate at their maximum output power for any temperature and solar radiation level. In this paper, we consider a photovoltaic panel supplying a battery. For maximizing the output power of this panel, we have using a boost dc/dc converter controlled by a PI regulator. For synthesizing this regulator, we have replaced the converter with an equivalent continuous model when we have considered the mean values, over the chopping period, of the electric quantities. Then, we have developed the transfer function of the system by using the small signal modeling around an optimal operating point. A PI synthesis has been achieved by using Bode method. In the study, we have taken into account the converter losses. Coefficients K_p and K_I obtained of PI regulator lead to good simulations. The theoretical results confirm excellent tracking effectiveness response. The regulator operates correctly on a large range.

Keywords: solar powerplants, photovoltaic panel, maximum power point tracking, boost dc/dc converter, losses

M. Salhi

Organization: Assist master in Sidi Mohamed Ben Abdellah University (USMBA), Higher School of Technology (EST), in Fèz, Morocco.
Education: – Diploma of thorough higher study (DESA) in automatic and systems analysis (2002-2004) from faculty of sciences dhar el-Mehrez at Sidi Mohamed Ben Abdellah University (USMBA).
– Researcher student in solar energy photovoltaic since January 2005.
Experience: Member of "Team research in electrical engineering, power electronics and renewable energies" (REEPER at the higher school of technology in Fez) belonging to the "Laboratory of electronics, signal-systems and data processing" (LESSI at the Faculty of Science in Fez).
Main range of scientific interests: renewable energy, optimal use of the photovoltaic power.
Publications: participation at congress on renewable energy; automatic control and systems engineering.

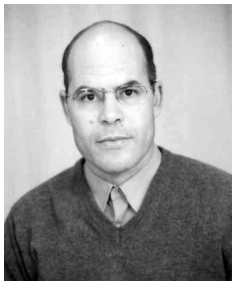

Rachid El-Bachtiri

Organization: Researcher teacher in Sidi Mohammed Ben Abdellah University (USMBA), Higher School of Technology (EST), in Fès, Morocco. Assisting Master (21/10/88). Ability Professor (22/01/97). Higher teaching Professor (22/01/01).
Education: Engineer (July 1988); Mohamed V University (Rabat), Mohammadia School of Engineers (EMI, 1983-1988), Electrical engineering, Electrotechnics and Industrial Electronics. Doctor of Sciences Applied (January 1997), Catholic University of Louvain (UCL, 1992-1997) at Louvain-La-Neuve (Belgium), Faculty of Science Applied (FSA), Department of electricity, Laboratory of electrotechnics and instrumentation (LEI).
Experience: Lectures and directed work: Power electronics and electrotechnics.
– Person in charge for a "Team of research in electrical engineering, power electronics and renewable energies" (REEPER at the higher school of technology in Fez) belonging to the: "Laboratory of electronics, signal-systems and data processing" (LESSI at the Faculty of Science in Fez).
Main range of scientific interests: electrical engineering and industrial electronics; resonance static conversion, effects of the harmonics, and their attenuation. Renewable energies; optimal use of the photovoltaic electrical power.
Publications: Papers in the power electronics and renewable energy field.

Ernest Matagne

Organization: Associate Professor in Université catholique de Louvain (UCL), Belgium, Assistant (1974), Senior staff member (1979), Associate professor (1999).
Education: Engineer (1971) in UCL, Doctor in Applied Sciences (1991).
Experience: Lectures and directed work in physics, electrical machines, power electronics, instrumentation and sensors, mechatronics, photovoltaic energy.
Main range of scientific interest: physics, analytical field computation, optimal design of electromechanical and electrical converters.
Publications: Physics, circuit theory, electrical machines, photovoltaic energy.

Introduction

Photovoltaic energy is a promising alternative energy source for the future, due to the world's limited conventional energy sources. Its disadvantages are that the initial cost is very high and the energy conversion efficiency is relatively low. Therefore, it is desirable to extract the highest possible power at any moment from the solar array source. The amount of power obtained from a photovoltaic array depends on its operating voltage. From its typical *V-I* and *V-P* characteristics (Fig. 1, *a* and *b* respectively), a unique operating point ($v = V_{mpp}$), known as the maximum power point (MPP), delivers the maximum available power $P_{\max}$. When operated at the MPP, the array is best utilized. The MPP of a photovoltaic array varies with irradiation, temperature and other effects. Up to now, a large variety of MPP seeking algorithms exists: look-up table [1, 2], perturbation and observation (P&O) [3], incremental conductance [4, 5] etc. Another maximum power point tracking (MPPT) is proposed in [6, 7], where a dc/dc converter is controlled so that $\partial I_{out}/\partial V$ and $\partial P/\partial V$ equal zero, where I_{out} and P are the dc/dc converter output current and input power respectively. However, these methods cannot take into account the losses in the dc/dc converter, particularly, the switch losses in the MOSFET transistor.

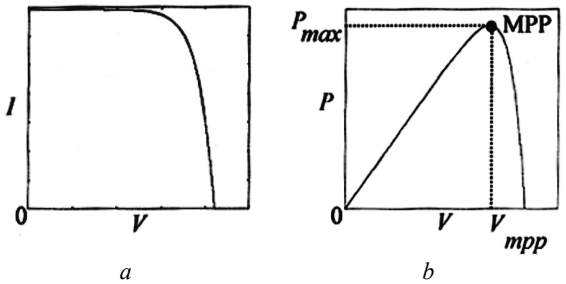

a *b*

Fig. 1. *Typical PV module: a – current-voltage and b – power-voltage characteristic*

In this paper, we pick up the work exposed in [7], and we consider that the dc/dc converter is not ideal. This converter is used between the PV and the battery to track the maximum power point of the PV module (Fig. 2, *a*).

The battery is considered as a constant voltage E in series with a constant resistance R_b [8, 9]. The MPP (V_{mpp}, P_{max}) is reached when $\partial P/\partial V = 0$, $P = VI$ being the PV power. Then, the control circuit must keep $(\partial P/\partial V)$ equals zero. That is possible with action on duty cycle α ($0 \le \alpha \le 1$) according to the solar irradiation λ and the temperature T. Duty cycle is a signal produced by a PI regulator. For synthesizing this regulator, we have developed a transfer function for the system using the small signal model. The coefficients K_p and K_i of the PI regulator are obtained by frequency synthesis.

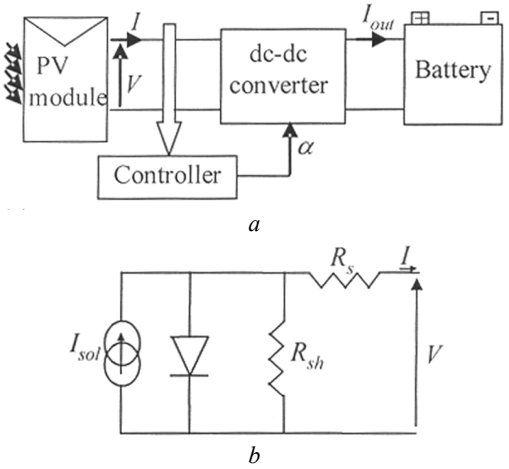

a

b

Fig. 2. *System bloc diagram (a) and – equivalent circuit(b) of a PV module*

Theoretical analysis

The power electronic converter is a boost converter inserted between the PV generator and the battery. It is characterised by its duty cycle α ($0 \le \alpha \le 1$) that gives the ratio input between the input and the output voltage when the conduction is continuous (Fig. 3).

The transistor is ON during αT and OFF during the rest of the period i.e. $(1 - \alpha)T$. The diode state, in continuous conduction, is complementary of the transistor one. The inductance is charged by the input through the transistor, and it discharges at the output through the diode.

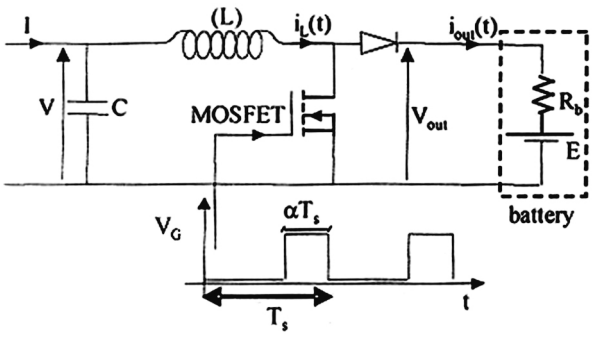

a

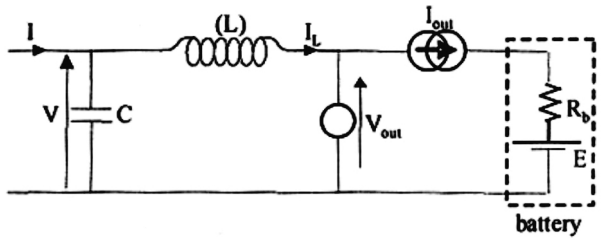

b

Fig. 3. *Boost converter (a); converter "mean" (b) equivalent circuit*

If the chopping frequency is sufficiently higher than the system characteristic frequencies, we can replace the converter with an equivalent continuous model. We will consider, for that, the mean values, over the chopping period, of the electric quantities (Fig. 3, *b*). The transistor can be replaced by a voltage source whose value equals its mean voltage. At the same, the diode can replaced by a current source.

Optimal operating point of PV module

The equivalent circuit of the PV module considered in this paper is shown in Fig. 2, *b*. The relationship between *V* and *I* is given by [10, 11]:

$$I - I_{sol} - I_{os}\left\{\exp\left[\frac{q}{\gamma kT}\left(V + R_s I\right)\right] - 1\right\} - \frac{V + R_s I}{R_{sh}}, \quad (1)$$

where:

$$I_{os} = I_{or}\left[\frac{T}{T_r}\right]^3 \exp\left[\frac{qE_{GO}}{\beta k}\left(\frac{1}{T_r} - \frac{1}{T}\right)\right] \quad (2)$$

$$I_{sol} = \left[I_{SC} + K_I\left(T - 298.18\right)\right]\frac{\lambda}{1000} \quad (3)$$

and *I* and *V* – cell output current and voltage, I_{or} – cell reverse saturation current, *T* – cell temperature in degree Kelvin, *k* – Boltzmann's constant (1.381e^{-23} J/K), *q* – electronic charge (1,602e^{-19} C), K_I – short-circuit current temperature coefficient at I_{sc} (= 0,0004 A/K), I_{sc} – short-circuit current at 25 °C and 1000 W/m^2, λ – solar irradiation in W/m^2, I_{sol} – light-generated current, E_{GO} – band gap for silicon (= 1.12 eV), γ (= β) – ideality factor (= 1,740), T_r – reference temperature (= 298,18 K), I_{or} – cell saturation current at T_r, R_{sh} – shunt resistance, R_s – series resistance.

The output power of PV panel is $P = VI$, at optimal point, we have:

$$\frac{\partial P}{\partial V} = I + V\frac{\partial I}{\partial V} = 0 \rightarrow \frac{\partial I}{\partial V} = \frac{-I}{V}. \quad (4)$$

Hence:

$$I = \left(V - R_s I\right)\left\{I_{os} A \exp\left[A\left(V + R_s I\right)\right] + \frac{1}{R_{sh}}\right\}, \quad (5)$$

where: $A = q/(\gamma kTN_{cell})$ and N_{cell} is the number of series cells in the module.

The PV module considered in this paper is the SM55. It has 36 series connected mono-crystalline cells. The manufacturer ratings of this PV photovoltaic under standard conditions (irradiation λ = 1000 W/m^2, A.M. 1.5, solar spectrum and cell temperature *T* = 25 °C) is shown in Table 1. The values of the rest parameters are as follow: R_s = 0,1124 Ω, R_{sh} = 6500 Ω and I_{or} = 4,842 μA.

Table 1

PV module specifications under standard test conditions (STC)

Cell temperature, °C	25
Open-cicuit voltage, V	21,7
Short-circuit current, A	3.45
Maximum power current, A	3.15
Maximum power voltage, V	17.4
Maximum power, W	55

Choice of *L* and *C*

The inductor value, *L*, required such the converter operates in the continuous conduction mode (Fig. 4, *a*) is calculated such that the peak inductor current at maximum input power does not exceed the power switch current rating [12]. Hence, *L* is calculated as:

$$L \geq \frac{V_{om}(1-\alpha_m)\alpha_m}{f_s\left|\Delta I_{Lm}\right|}, \quad (6)$$

where f_s (= $1/T_s$) – switching frequency, α_m – duty cycle at maximum converter input power, ΔI_{Lm} – peak-to-peak ripple of the inductor current, V_{om} – maximum of dc component of the output voltage, I_{om} – dc component of the output current at maximum output power.

Taking into account that the ripple of the PV output current must be less than 2 % of its mean value [12], the input capacitor value is calculated to be:

$$C \geq \frac{I_{om}\alpha_m^2}{0.02(1-\alpha_m)V_{mn}f_s}, \quad (7)$$

where V_{inm} – PV input voltage at the maximum power point.

When the boost converter is used in PV applications, the input power, voltage and current change continuously with atmospheric conditions. Thus, the converter conduction mode could change since it depends on them. Also, the duty cycle α is changed continuously in order to track the maximum power point of the PV array. The choice of the converter switching frequency and the inductor value is a compromise between the converter efficiency, the cost, the power capability and the weight. For example, higher is the switching frequency, lower is the inductor core size, but the power switch losses increase. Also, by using a large L value, the peak-to-peak current ripple ΔI_L is smaller; requiring lower current rating power switches. But the converter size is increased substantially because a larger inductor core is required.

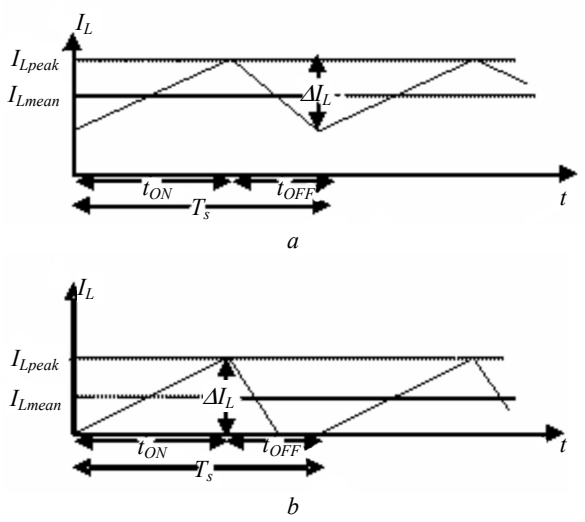

Fig. 4. *Boost converter waveforms: (a) continuous conduction mode and (b) discontinuous conduction mode*

Losses in the MOSFET transistor

In this study, we have taken into account the losses in the MOSFET transistor for determining the power transmitted to the battery at the optimal operating point. At ON state (Fig. 5), the transistor is equivalent to the R_{DSon} resistance. This resistance is considered as a constant. The average switching power dissipation in dc/dc converter is given as follow [13]:

$$P_{on-off} = \frac{1}{2} V_{DS} I_{DSon} \frac{t_{cON} + t_{cOFF}}{T_s} = \\ = \frac{1}{2} V_{DS} I_{DSon} f_s \left(t_{cON} + t_{cOFF} \right), \quad (8)$$

where:

$$V_{DS} = E + V_s + R_b I_{out}, \quad V_{DSon} \approx I_L, \quad t_{cON} = t_{ri} + t_{fv} \\ t_{cOFF} = t_{rV} + t_{ft} \quad (9)$$

and P_{on-off} – switching losses, V_{DS} – drain-to-source voltage, I_{DSon} – drain-to-source current, t_{ri} – rise time of transistor current, t_{fv} – fall time of the voltage, t_{rv} – rise time of the voltage, t_{ft} – fall time of current at the state OFF.

The switching power losses in the diode are neglected. And

$$P_d \approx R_{DSon} I_{DSon}^2 \alpha + V_s I_{out} + r_L I_L^2, \quad (10)$$

where P_d – average power dissipation in dc/dc converter, R_{DSon} – static drain-to-source on-resistance, α_{mpp} – duty cycle at MPP, V_s – threshold voltage of diode, I_D – average current of diode, r_L – resistance of inductor, I_L – average current of inductor.

So, the output power of dc/dc converter at optimal operating point (P_{out}) is:

$$P_{out} = P_{mpp} - (P_{on-off} + P_d), \quad (11)$$

where P_{mpp} – maximum power point.

The efficiency (η) of dc/dc converter is defined as:

$$\eta = \frac{P_{out}}{P}. \quad (12)$$

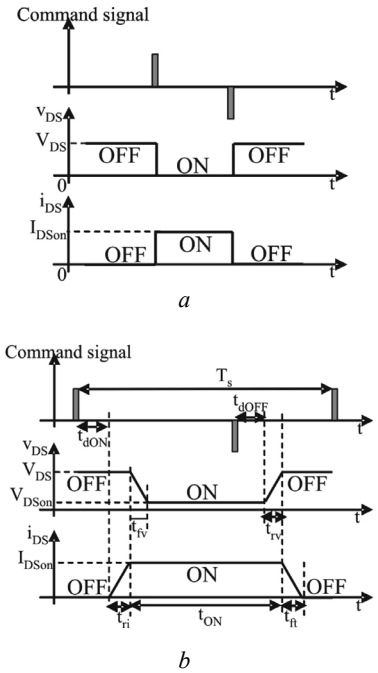

Fig. 5. *Switching time: a – ideal waveforms and b – real waveforms*

Frequencial synthesis of PI regulator

We deduce from the continuous model equations (Fig. 3, *b*) the following equations:

$$C \frac{dV}{dt} = I - I_L \quad (13)$$

$$V = L\frac{dI_L}{dt} + r_L I_L + V_{out} \quad (14)$$

$$I_{out} = (1 - \alpha) I_L, \quad (15)$$

where:

$$V_{out} = R_{DSon}\alpha I_L + R_b(1 - \alpha) I_L + (E + V_s)(1 - \alpha) \quad (16)$$

and r_L – inductor resistance, R_b – battery resistance, V_s – threshold voltage of the diode.

For expanding in series equations (11-14) around an optimal operating point, we write: $q = q_{mpp} + \Delta q$, for each quantity q in the set $\{V, \alpha, I_L, I, I_{out}\}$ defining the operating point. So, the equations system become:

$$C\frac{d\Delta V}{dt} = \Delta I - \Delta I_L \quad (17)$$

$$L\frac{d\Delta I_L}{dt} = \Delta V - \left(r_L + \alpha_{mpp} R_{DSon}\right)\Delta I_L - \\ - R_b \Delta I_{out} + \left(E + V_s - R_{DSon} I_{lmpp}\right)\Delta\alpha \quad (18)$$

$$\Delta I_{out} = \left(1 - \alpha_{mpp}\right)\Delta I_L - I_{Lmpp}\Delta\alpha \quad (19)$$

At steady state, we have:

$$I_{mpp} = I_{Lmpp} \quad (20)$$

$$V_{mpp} = \left(r_L + \alpha_{mpp} R_{DSon}\right) I_{Lmpp} + \\ + R_b \Delta I_{outmpp} + \left(E + V_s\right)\left(1 - \alpha_{mpp}\right) \quad (21)$$

$$I_{outmpp} = \left(1 - \alpha_{mpp}\right) - I_{Lmpp} \quad (22)$$

For a small variation around an optimal operating point, the system can be shown by a functional diagram like that used in [14] for synthesizing the regulator. Thus, the system can be presented as (Fig. 6):

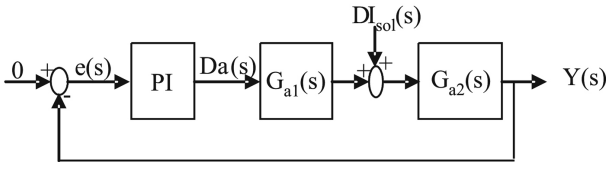

Fig. 6. *Functional diagram of the system*

According to [14], the transfer function $G_{a1}(s)$ and $G_{a2}(s)$ must have the following form:

$$G_{a1}(s) = K_{a1}\frac{R_{a1}(s)}{s^{\alpha_1}} \text{ and } G_{a2}(s) = K_{a2}\frac{R_{a2}(s)}{s^{\alpha_2}}, \quad (23)$$

where $R_{a1}(s)$ and $R_{a2}(s)$ – rational fractions with $R_{a1}(0) = R_{a2}(0) = 1$, K_{a1} and K_{a2} – static gains of $G_{a1}(s)$ and $G_{a2}(s)$, α_1 and α_2 – integration numbers of $G_{a1}(s)$ and $G_{a2}(s)$ respectively.

In this paper, we have obtained:

$$K_{a1} = \frac{\left(K_1 G - K_2\right)\left(1 + R_s G_m\right)\left\{E + V_s + \left(R_b - R_{DSon}\right) I_{Lmpp}\right\}}{K_1 + K_2 K_3} \quad (24)$$

$$K_{a2} = \frac{K_1 + K_2 K_3}{\left(1 + R_s G_m\right)\left(1 + GK_3\right)} \quad (25)$$

$$R_{a1}(s) = \frac{1}{\frac{K_1 LC}{K_1 + K_2 K_3}s^2 + \frac{K_1 K_3 C + K_2 L}{K_1 + K_2 K_3}s + 1} \quad (26)$$

$$R_{a2}(s) = \frac{\frac{K_1 LC}{K_1 + K_2 K_3}s^2 + \frac{K_1 K_3 C + K_2 L}{K_1 + K_2 K_3}s + 1}{\frac{LC}{1 + GK_3}s^2 + \frac{GL + GK_3}{1 + GK_3}s + 1}, \quad (27)$$

where:

$$K_1 = 1 + \frac{AR_s\left(R_s I_{mpp} - V_{mpp}\right)}{R_{dm}\left(1 + R_s G_m\right)},$$

$$K_2 = \frac{A\left(R_s I_{mpp} - V_{mpp}\right)}{R_{dm}\left(1 + R_s G_m\right)} - G$$

$$K_3 = r_L + \alpha_{mpp} R_{DSon} + R_b\left(1 - \alpha_{mpp}\right),\ G = \frac{G_m}{1 + R_s G_m},$$

$$G_m = \frac{1}{R_{dm}}, \text{ and } R_{dm} = \frac{1}{I_{os} A \exp\{A(V_{mpp} + R_s I_{mpp})\}}.$$

K_{a1} and K_{a2} are constants for a given temperature T and solar irradiation λ.

The transfer function of the open loop used to synthesizing a PI regulator is:

$$G_0(s) = G_{a1}(s) G_{a2}(s) = \\ = \frac{\left(K_1 G - K_2\right)\left\{E + V_s + \left(R_b - R_{DSon}\right) I_{Lmpp}\right\}}{1 + GK_3} \times \\ \times \frac{1}{\frac{LC}{1 + GK_3}s^2 + \frac{GL + CK_3}{1 + GK_3}s + 1} \quad (28)$$

Simulation procedure

The bloc used for simulations is given by Fig. 7, *a*. In PV module block, equations (1-3) are used; and in block (converter + battery) equations (11-14) are used. The switching losses are cutting off the output converter power according to equations (8-11).

The proposed controller circuit that forces the system to operate at its optimal operating point under variable temperature and insolation conditions, is shown in Fig. 7, *b*. On one hand, we multiply the PV output current I by the PV output voltage V. Then, we obtain the PV output power P who is derived in order to obtain the (dP/dt) signal. On the other hand, we drive the signal voltage and invert it. Thus, the signal $1/(dV/dt)$ is obtained.

The product of 1/(*dV*/*dt*) by (*dP*/*dt*) signals gives the (*dP*/*dV*) signal, who is compared to zero. The resulting difference signal (error signal) is the input signal of the PI regulator. This PI regulator is used to regulate the duty cycle signal of the *dc*/*dc* converter until that the condition: *dP*/*dV* = 0 is satisfied.

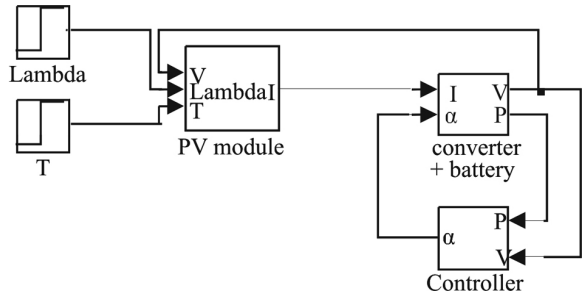

a

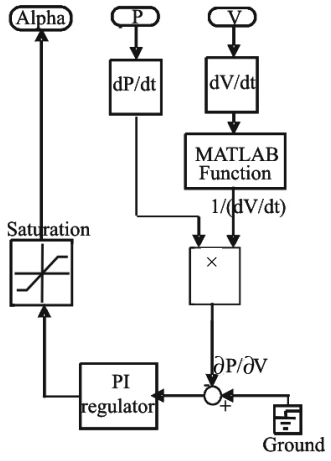

b

Fig. 7. *a – bloc diagram for system and b – MPPT tracker circuit*

Results and discussion

Theoretical results

The battery voltage, the threshold voltage of the diode, the resistance of battery and the series resistance of the inductor, used in this paper, are respectively $E = 24$ V, $V_s = 0.7$ V, $R_b = 0.65$ Ω and $r_L = 0.05$ Ω. The MOSFET transistor utilized here, is an IRFP250. Their characteristics used in this paper are: $R_{DSon} = 0.085$ Ω, $t_{fv} = 86$ ns, $t_{rv} = 62$ ns, $t_{ri} = 16$ ns and $t_{ft} = 70$ ns. Fifty kilohertz switching frequency is used.

The PI controller gain and the integral time constant obtained by frequency synthesis using Bode method are respectively $K_p = 0.01$ and T_i ($= 1/K_i$) = 1.8 ms. Using equation (6), the boost inductance choice is $L = 1$ mH. With equation (7), the choice of input capacitance is $C = 4.7$ μF.

For different values of irradiation λ and temperature T, the computation of the theoretical optimum quantities V_{mpp}, P_{mpp}, P_{out} and η are assembled in Table 2.

Table 2

Theoretical quantities V_{mpp}, P_{mpp}, P_{out} and η for different values of λ and T

Values of λ (W/m^2) and T (K)	**Optimum voltage V (V)**	**Optimum power P (W)**	**Optimum power P_{out} (W)**	**Efficiency η (%)**
λ = 100 and T = 298.18	14.25	4.393	4.224	96.16
λ = 1000 and T = 298.18	17.39	54.80	52.07	95.01
λ = 1000 and T = 320.18	15.65	48.61	46.07	94.76
λ = 100 and T = 320.18	12.31	3.715	3.570	96.11

Simulation results

The simulation study was made to illustrate the response of the proposed method to rapid temperature and solar irradiance change. For this purpose, the irradiance λ and the temperature T, which are initially 100 W/m^2, and 298.18 K, are switched, at 0.02 s and 0.05 s, to 1000 W/m^2 and 320.18 K respectively (Fig. 8, *a* and *b*). and vice versa (Fig. 9 *a* and *b*), i.e., the solar irradiance changes from 1000 W/m^2 to 100 W/m^2 at 0.02 s and the temperature changes from 320.18 K to 298.18 K at 0.05 s.

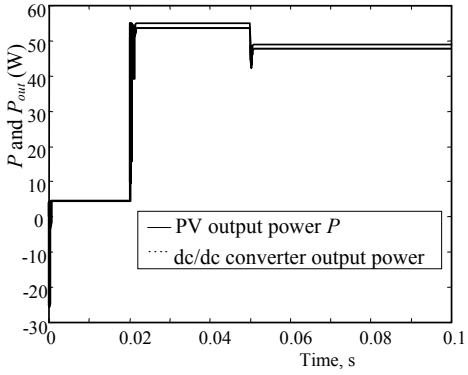

a

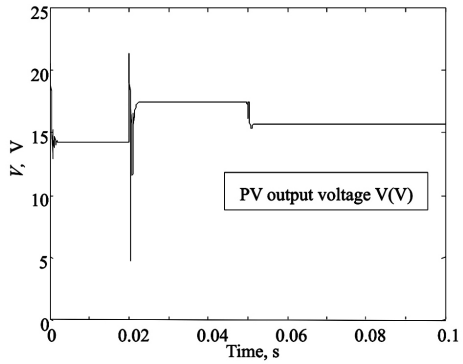

b

Fig. 8. *Variation of: a – PV output power and dc/dc converter output power, and b – PV output voltage for a step change on irradiation and temperature from 100 W/m^2 to 1000 W/m^2 and 29818 K to 320.18 K respectively*

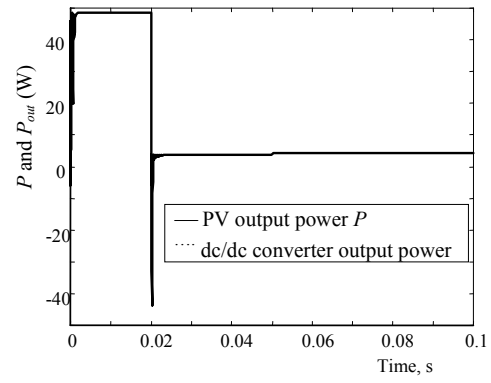

a

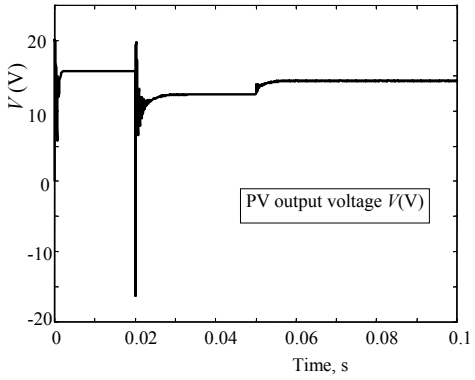

b

Fig. 9. *Variation of: a – PV output power and dc/dc converter output power; b – PV output voltage for a step change on irradiation and temperature from 1000 W/m² to 100 W/m² and 320.18 K to 298.18 K respectively*

In Fig. 8, *a* and 9, *a* the variation of instantaneous PV power *(P)* and dc/dc converter output power for a step change of temperature and solar irradiance are shown. And the Fig. 8, *b* and 9, *b* give the variation of PV output voltage for a step change of temperature and solar irradiance.

The optimum values of PV output voltage, instantaneous PV power and dc/dc converter output power obtained by simulations are assembled in Table 3.

Table 3

Simulated quantities V_{mpp}, P_{mpp}, P_{out} and η for different values of λ and T

Values of λ (W/m²) and T (K)	**Optimum voltage V (V)**	**Optimum power P (W)**	**Optimum power P_{out} (W)**	**Efficiency η (%)**
λ = 100 and T = 298.18	14.25	4.396	4.205	96.66
λ = 1000 and T = 298.18	17.41	54.83	51.99	94.82
λ = 1000 and T = 320.18	15.66	48.64	45.95	94.47
λ = 100 and T = 320.18	12.31	3.717	3.549	95.48

To watch Tables 2 and 3, then Fig. 8 and 9, it is clear, on one hand, that the average voltage (V), instantaneous PV power (P) and dc/dc converter output power (P_{out}) are very close to their optimal values V_{mpp}, P_{mpp} and P_{outmpp}. And on the other hand, the values obtained by simulation coincide with their obtained by programming.

The losses in the dc/dc converter varies from 0.168 W to 3.04 W for λ =100 W/m², T = 320.18 K, and λ = 1000 W/m², T = 298.18 K respectively. They can be minimized for adequate choices of the component of dc/dc converter.

The simulations of the MPPT show that the system is stable. The oscillations about the computed optimal operating point are due to the switching action of the dc/dc converter. The transients between operating points are natural for a dynamic system which is controlled by a PI type controller.

Conclusion

In this paper, a method that forces a photovoltaic panel to operate at its maximum power point under variable temperature and irradiation conditions is developed. This method is tested by simulations in Matlab software. It has been concluded that the method was able to track the irradiance and the temperature level change rapidly. The PI regulator used in this work for controlling the boost dc/dc converter in order to get the system operating at the PV maximum power is synthesized by frequencial synthesis using Bode method. So, we have developed a transfer function of global model using a small signal method by taking into account the losses in the dc/dc converter. Simulations show that the regulation is robust against disturbances.

References

1. Hohm D., Ropp M. Comparative study of maximum power point tracking algorithms // Progr. photovoltaics: Res. Appl. 2003. No. 11. P. 47-62.

2. Salas V., Manzanas M.J., Lazaro A. The control strategies for photovoltaic regulators applied to stand-alone systems // 28th annual conference of the IEEE Industrial Electronics Society, Sevilla. 2002. Vol. 4. P. 3274-3279.

3. Kislovski A., Redl R. Maximum power-tracking using positive feedback // Proceedings of IEEE Power Electronics Specialist Conference. 1994. P. 1065-1068.

4. Wolf S., Enslin J. Economical, PV maximumpower point tracking regulator with simplistic controller // Proceedings of IEEE Power Electronics Specialist Conference. 1993. P. 581-587.

5. Hiyama T., Kitabayashi K. Neural network based estimation of maximum power generation // IEEE Trans. Energy Convers. 1997. Vol. 12. P. 241-247.

6. Salhi M., El-Bachtiri R. A PI regulator synthesis for tracking the optimal operating point of photovoltaic system supplying a battery // World renewable energy

congress IX (WREC-IX), RT 15 (CD proceeding). Florence. Italy. 19-25 August. P. 515 (abstract), 2006.
7. Salhi M., El-Bachtiri R., Matagne E. Boost dc/dc converter control for tracking the maximum power of PV system supplying a battery // Conference on Systems and Control (CSC). Marrakech, Morocco, May 16-18, 2007.
8. Min Chen, Gabriel A. Rincon-Mora. Accurate Electrical Battery Model capable of Predicting Runtime and I-V Performance // IEEE Transactions on Energy Conversion. June 2006. Vol. 21. No. 2. P. 504-511.
9. Eakburanawat J., Boonyaroonate I. Development of a thermoelectric battery-charger with Microcontroller-based maximum power point tracking technique // Applied Energy. 2006. Vol. 83. P. 687-704.
10. Vachtsevanos G., Kalaitzakis K. A hybrid photovoltaic simulator for utility interactive studies // IEEE Trans. Energy Conv. June 1987. Vol. EC-2. P. 227-231.
11. Jaboori M.G., Saied M.M., Hanafy A.A. A contribution to the simulation and design optimization of photovoltaic systems // IEEE Trans. Energy Conv. Sept 1991. Vol. 6. P. 401-406.
12. Mohan N. et al. Power Electronics-Converters, Applications and Design. New York: Wiley, 1989.
13. Salhi M., El-Bachtiri R. Evaluation des pertes dans un convertisseur dc/dc utilisé pour la poursuite du point à puissance maximale dans un panneau photovoltaique alimentant une batterie // Colloque international sur les energies renouvelables (CER'2007). Oujda, Maroc. 4-5 Mai. 2007.
14. Maret L. Regulation automatique. Lausanne: Presses polytechniques romandes, 1987.